

EFFECT OF CALCINATION TEMPERATURE VARIATION ON GREEN SYNTHESIS OF CADMIUM SULFIDE FOR CIPROFLOXACIN PHOTODEGRADATION

Aminatul Haq Faizah ¹, Gunawan ¹  , Khabibi ¹, Roni Adi Wijaya ¹

¹ Department of Chemistry, Diponegoro University, Semarang, 50275, Indonesia



Received 22 April 2024
Accepted 27 May 2024
Published 30 June 2024

Corresponding Author

Gunawan, gunawan@live.undip.ac.id

DOI

[10.29121/granthaalayah.v12.i6.2024.5681](https://doi.org/10.29121/granthaalayah.v12.i6.2024.5681)

Funding: This research received no specific grant from any funding agency in the public, commercial, or not-for-profit sectors.

Copyright: © 2024 The Author(s). This work is licensed under a [Creative Commons Attribution 4.0 International License](https://creativecommons.org/licenses/by/4.0/).

With the license CC-BY, authors retain the copyright, allowing anyone to download, reuse, re-print, modify, distribute, and/or copy their contribution. The work must be properly attributed to its author.



ABSTRACT

The green synthesis method has been successfully carried out to CdS with tea leaf extract and calcination temperature variation for the application of photocatalytic degradation of ciprofloxacin antibiotic. Variations in calcination at temperatures of 500, 600, and 700 °C were carried out to determine the effect of temperature on morphology and elemental composition, crystal structure and size, functional groups, and band gap energy by SEM-EDX, XRD, FTIR, and UV-DRS Spectrophotometer. The SEM-EDX image of the synthesized CdS is smooth and spherical and there is agglomeration with an even distribution of elements. The results of XRD and FTIR characterization showed the CdS peaks. The size of the CdS crystal increased with increasing temperature, namely CdS-600 at 64 nm and CdS-700 at 81.58 nm. The band gap energy value is influenced by the calcination temperature during synthesis with the band gap energy values of CdS-600 2.3 eV and CdS-700 2.38 eV. The percentage of CdS effectiveness with variations in calcination temperature in ciprofloxacin photodegradation is CdS-500 at 32.18%, CdS-600 at 48.72%, and CdS-700 at 8.73%. The optimum condition of CdS synthesis in degrading ciprofloxacin by photocatalytic process occurs at a temperature of 600°C with a photocatalytic irradiation time under visible light for 120 minutes, a CdS mass of 10 mg, and an initial concentration of ciprofloxacin of 25 ppm. This result demonstrates the potential of an environmentally friendly method that can be applied in wastewater treatment.

Keywords: Cadmium Sulfide, Green Synthesis, Calcination, Photocatalytic, Ciprofloxacin

1. INTRODUCTION

Ciprofloxacin (CIP) is a third-generation fluoroquinolone antibiotic, which is widely used to treat bacterial infections due to its broad spectrum of antibacterial activity (i.e., it can inhibit both gram-negative and gram-positive bacteria). On the other hand, excessive use of CIP can pose a serious threat to the ecosystem such as antibiotic resistance [Kelly & Brooks \(2018\)](#), [Mathur et al. \(2021\)](#). Consumption of water contaminated by ciprofloxacin in the environment can cause health problems such as vomiting, headaches, diarrhoea, skin disorders, and the immune system [Gunawan et al. \(2023\)](#), [Shehu Imam et al. \(2018\)](#). Organic contamination in waters

originating from the pharmaceutical industry often contains toxic pollutants with low biodegradability Barra Caracciolo et al. (2015), Chopra & Kumar (2017), Dsikowitzky & Schwarzbauer (2014), so an efficient method is needed to overcome this problem.

Various methods are carried out to overcome organic pollutants in waters such as bioremediation and coagulation-flocculation followed by the activated sludge biological process Kumar et al. (2023), Majumder et al. (2014). This method still has shortcomings compared to photocatalytic. The semiconductor photocatalytic method is considered one of the promising methods for CIP degradation in water because it is environmentally friendly, has low energy consumption, low cost, and has no secondary pollutants Zhao et al. (2021), Zhao et al. (2021). Another advantage is that the photocatalytic reaction is a non-specific reaction, meaning it can destroy organic compounds widely ranging from alkanes, alkenes, alcohols, phenols, carboxylic acids, aromatic compounds, dyes, pesticides, to surfactants. In addition, photocatalysis can degrade organic compounds because it has a very strong oxidation power Akerdi & Bahrami (2019).

The photocatalytic activity comes from a hydroxyl radical resulting from an electron-hole pair (e^-/h^+), an electron-hole pair e^-/h^+ is produced when the photon energy exceeds the band gap value, electrons (e^-) then settle in the conduction band (CB) after leaving their place in the valence band (VB) producing holes (h^+) in the valence band Gunawan et al. (2023), Verma & Singh (2023). Photocatalytic activity depends on semiconductor characteristics, where the photocatalytic properties can be modified through the techniques and methods used for synthesis to control particle size and shape.

Cadmium sulfide (CdS) is a semiconductor compound with a band gap of 2.4 eV which is suitable and excellent in photocatalytic activity due to its visible light absorption feature. The photocatalytic activity of CdS is influenced by the synthesis conditions, structure, morphology, particle size, surface area, and crystallinity Lang et al. (2014). CdS displays efficient visible light absorption at wavelengths up to 530 nm Shen et al. (2013). CdS is easy to synthesize, one of which is by the green synthesis method.

The synthesis of cadmium sulfide by the green synthesis method is now starting to be developed because it is cost-effective, harmless, and environmentally friendly. Several biological entities that can play a role in the green synthesis method to produce nanoparticles include algae, fungi, microbes, actinomycetes, and plant extracts. Each of these agents has its advantages. Compared to other agents, tea extract used as a component in green synthesis acts as a complexing agent that regulates the size of cadmium sulfide in the form of more stable nanoparticles Shivaji et al. (2018).

Efforts to increase the photocatalytic effectiveness of semiconductors can be calcined to increase light absorption and charge separation processes during the reaction. Increasing the calcination temperature will affect the increase in crystal size. In addition, heating with high temperature can also affect the band gap energy so that it can increase photocatalytic activity Asadah et al. (2022). Therefore, in this study, the synthesis of green semiconductor CdS with tea leaf extract with calcination temperature variation was carried out for the application of photocatalytic degradation of ciprofloxacin antibiotic. Calcination variations at 500, 600, and 700 °C were carried out to determine the effect of temperature on crystal size, crystallinity, and band gap energy. Morphology and elemental composition, crystal structure and size, functional groups, and band gap energy of the synthesized CdS were characterized by SEM-EDX, XRD, FTIR, and UV-DRS spectrophotometer.

The results of this study are expected to provide new insights into developing more efficient and environmentally friendly photocatalysts for wastewater treatment applications.

2. EXPERIMENTS

2.1. MATERIALS AND INSTRUMENTS

Trade tea powder, Cadmium sulfate octahydrate ($3\text{CdSO}_4 \cdot 8\text{H}_2\text{O}$) (Merck), sodium sulfide (Na_2S) (Loba Chemie), methanol (Merck), deionized water (Waterone), acetone, distilled water, ciprofloxacin (Sigma Aldrich). The instruments used are glassware (Herma), filter paper (Whatman no.42), 1 mL volume pipette (Iwaki), analytical balance (Ohaus, Model PA323), oven, furnace (Nabertherm), hotplate (Thermo Scientific Cimarec), centrifuge (Hettich Zentrifugen), photocatalytic reactor with visible light (Vaco IP 66, 200 W), UV-Vis spectrophotometer (Shimadzu UV-1280), UV-DRS spectrophotometer (Shimadzu UV-2450), Scanning Electron Microscope (JSM-6510LA), Energy Dispersion X-Ray Spectroscopy (JED-2300 Analysis Station Plus), X-Ray Diffraction (Shimadzu 7000), and FTIR Spectrophotometer (PerkinElmer Frontier).

2.2. GREEN SYNTHESIS OF CADMIUM SULFIDE

The synthesis was carried out by dissolving 3.848 grams of $3\text{CdSO}_4 \cdot 8\text{H}_2\text{O}$ and 0.39 grams of Na_2S each in a 10 mL volumetric flask using distilled water to obtain a solution of 0.5 M CdSO_4 and 0.5 M Na_2S . The solution was stored in vials for further use. 0.5 grams of tea powder was mixed in 30 mL of methanol and left in the dark for 1 day, after 1 day filtering was done to separate the tea precipitate from the solution. The extract was added to 2 mL of 0.5 M CdSO_4 solution and left in the dark for 3 days, followed by the addition of 0.5 mL of 0.5 M Na_2S solution and left in the dark for 4 days. The precipitate was washed with deionized water and centrifuged at 6000 rpm for 10 minutes then dried on a hotplate at 70°C .

2.3. DETERMINATION OF TEMPERATURE CALCINATION VARIATION

The calcination process was carried out at temperature variations of 500, 600, and 700°C for 2 hours each, which were then named CdS-500; CdS-600; and CdS-700. The process started by putting the samples into a vacuum furnace instrument at a constant time for 60 minutes.

2.4. CHARACTERIZATION

The synthesized CdS samples were characterized using a Scanning Electron Microscope-Energy Dispersive X-ray (SEM-EDX) instrument to determine the morphology and elemental composition. Meanwhile, X-ray diffraction (XRD) to determine the crystal structure and a UV-DRS Spectrophotometer to determine the band gap. In addition, the difference in functional groups of CdS was observed by Fourier Transform Infrared (FTIR).

2.5. PHOTOCATALYTIC TEST

Photodegradation applications were carried out with 100 mL of 25 ppm ciprofloxacin solution added with 10 mg of CdS semiconductor catalyst and mixed

in dark conditions for 1 hour to achieve adsorption-desorption equilibrium. It was illuminated with visible light and stirred with a magnetic stirrer at time intervals of 15; 30; 45; 60; 75; 90; 105; and 120 minutes. The solution was centrifuged at 5000 rpm for 5 minutes before measuring the absorbance of ciprofloxacin solution after photocatalytic with UV-Vis spectrophotometer at 319 nm wavelength.

3. RESULT AND DISCUSSION

3.1. GREEN SYNTHESIS OF CDS

The synthesis of green CdS was carried out using tea leaves that had previously been tested for flavonoids with the results in 0.01 g of tea containing 0.41% flavonoid quercetin. Predicted reactions that occur in the mechanism of green cadmium sulfide synthesis are described in Figure 1. Phytochemical screening is carried out first to determine the presence or absence of alkaloids, flavonoids, phenols, tannins, quinones, saponins, etc. Quercetin can chelate metal ions (Cd^{2+}) to form metal complexes Dolatabadi (2011). The cadmium complex with quercetin is formed by the way quercetin acts as a capping agent which then can also protect Cd from bulk and against aggregation so that when the addition of S^{2-} ions from Na_2S can form nano-sized CdS crystals Zhou et al. (2014).

Figure 1

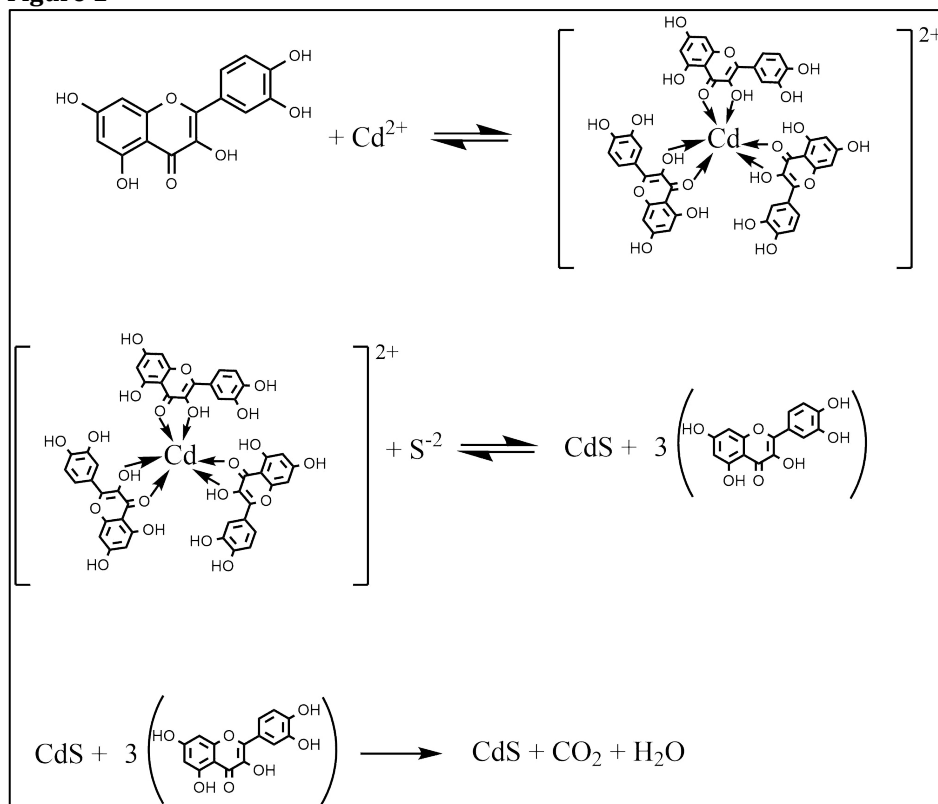


Figure 1 CdS Formation Reaction by Green Synthesis Method

3.2. CHARACTERIZATION

3.2.1. MORPHOLOGY AND ELEMENTAL COMPOSITION

The semiconductor catalysts that were characterized were CdS powder calcined at 600 °C and 700 °C while SEM images at 1000x, 5000x, 7500x, and 10000x magnifications are given in Figure 2. Based on the SEM characterization results of

the CdS-600 sample at 5000x magnification, it can be seen that the morphology of the particles is smooth and round and there is agglomeration. The CdS-700 sample SEM characterization results at 1000x magnification showed a less smooth spherical change with non-uniform size and agglomeration. The spherical morphology and small particle size are expected that the synthesized cadmium sulfide has good photocatalytic activity. In the case of biogenic synthesis based on plant extracts, nanoparticles are generally formed that are very stable and homogeneous in shape [Shivaji et al. \(2018\)](#). In addition, [Figure 3](#) is the result of mapping or elemental distribution of samples tested with the different colouring of each element. Both CdS-600 and CdS-700 samples have an even distribution of elements.

Figure 2

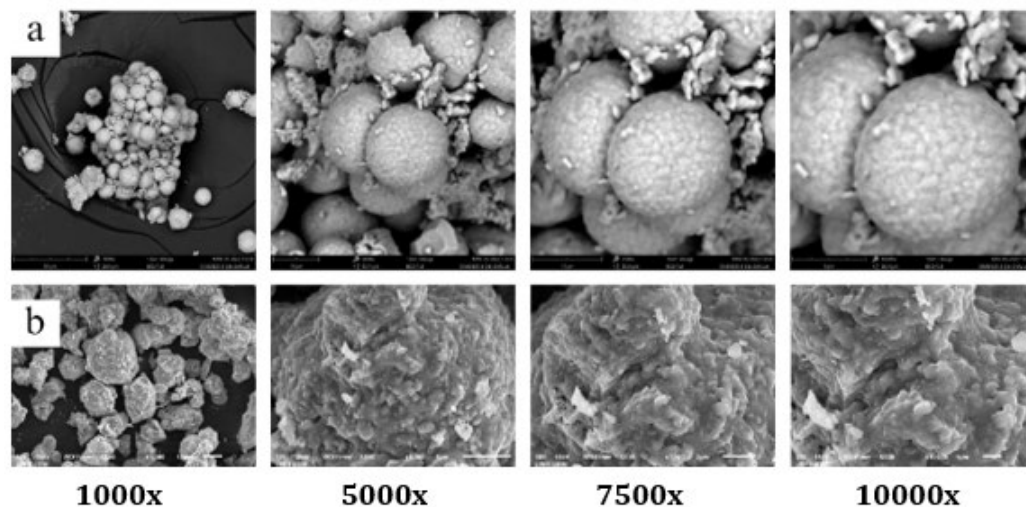


Figure 2 SEM Morphology of a) CdS-600 b) CdS-700

Figure 3

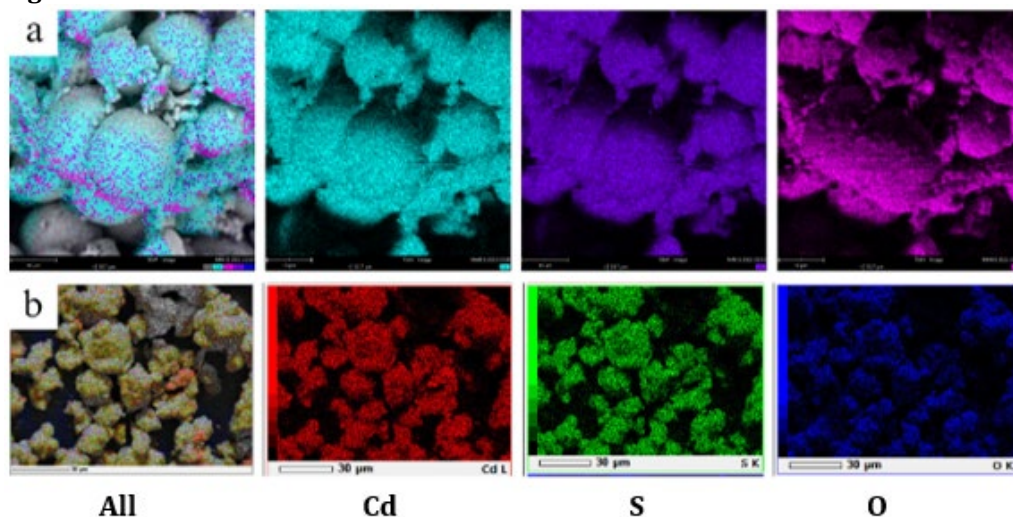


Figure 3 Surface Metal Mapping of a) CdS-600 b) CdS-700

The EDX analyzer results of both samples prove that there are elements of the constituent elements of cadmium sulfide, namely Cd and S, so it can be concluded that cadmium sulfide has been synthesized properly as shown in [Table 1](#). The CdS-600 sample contained the element C which was thought to come from the carbon

tab used to attach the sample during EDX testing. The O element that appears with a large enough percentage is caused by air during the calcination process. The presence of additional oxygen peaks in the EDX spectra may come from the organic capping material i.e. tea extract bound to the surface. Another possibility for the presence of elemental oxygen is due to calcination occurring in atmosphere conditions. [Shivaji et al. \(2018\)](#).

Table 1

Table 1 Shows the Atomic Element Content on the Surface of Each CdS Sample

Sample	Element	Weight Concentration (%)
CdS 600	Cd	48,18
	O	38,23
	S	9,47
	C	4,13
CdS 700	Cd	44,41
	S	11,53
	O	44,06

3.2.2. CRYSTALLINITY ANALYSIS

To examine the crystal size and phase structure, XRD testing of CdS nanoparticle structures prepared by green synthesis at different temperatures was carried out. The test was conducted using $K\alpha$ radiation from a copper anode (Cu- $K\alpha$) with a wavelength of 0.154 nm and recorded at a diffraction angle of 2θ between 10 - 90° . The diffractogram of the measurement results in the form of diffraction peaks with a certain intensity was then compared with the standard data obtained from Crystallography Open Database (COD) No. 1011054 shown in [Figure 4](#).

Figure 4

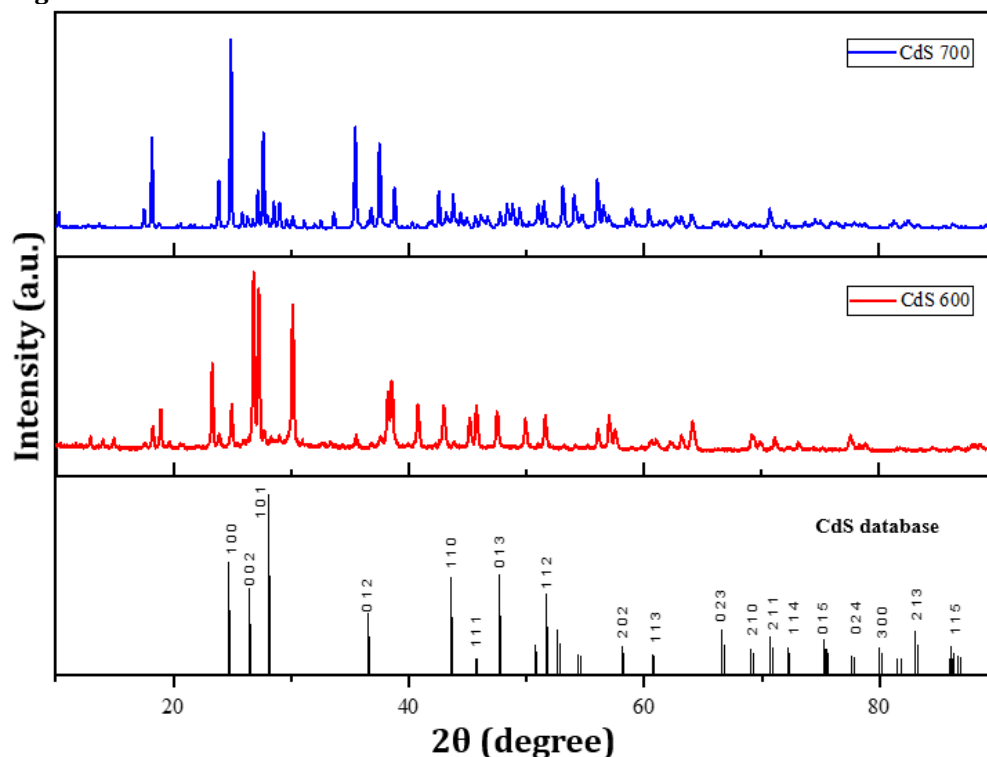


Figure 4 XRD Spectrum CdS-600 dan CdS-700

The XRD pattern results of the measured samples show that cadmium sulphide (CdS) has been formed which is characterised by the formation of diffraction peaks with high intensity, this proves that the crystallinity of the synthesised CdS sample is quite good [Asadah et al. \(2022\)](#). Diffractogram peaks with the highest intensity of CdS-600 and CdS-700 samples are shown in [Table 2](#). The peak intensity of the diffractogram increases with increasing synthesis temperature, The increase in the intensity of various peaks indicates better crystallinity which leads to a decrease in the strain value and dislocation density [Chauhan \(2020\)](#). The synthesised CdS has a crystal phase with a p-63mc space group, which is hexagonal. To maintain excellent optoelectronic properties, CdS must remain in the hexagonal wurtzite structure [Xiao et al. \(2014\)](#). The crystal size was calculated based on the Full Width at Half Maximum (FWHM) values at various peaks with the Debye-Scherrer equation (1) [Gunawan et al. \(2022\)](#).

$$G = \frac{k \lambda}{D \cos \theta} \quad (1)$$

Where G is the crystal size, k = 0.9 is the formation factor, λ is the wavelength of the CuK α line, D is the FWHM in radians, and θ is the Bragg angle.

The crystal size increases with increasing synthesis temperature, the crystal size of CdS-600 is 64 nm to CdS-700 of 81.58 nm and it can be concluded that the synthesized CdS includes nanoparticles. Crystal grains undergo a growth process when CdS is calcined. If the temperature used is a temperature that exceeds the optimum temperature, the crystals will be larger. If the temperature used is below the optimum temperature, it is possible that the expected crystals have not formed or even formed but are not pure [Aprilianingrum \(2016\)](#). The higher calcination temperature causes the crystal size and per cent crystallinity to be greater. This is because high temperatures make particles move more reactive and faster than low temperatures and result in agglomeration [Asadah et al. \(2022\)](#).

Table 2

Table 2 XRD Result Analysis of CdS-600 and CdS-700			
Sample	2 θ	h k l	d (nm)
	24,95	(1 0 0)	43,74
	26,44	(0 0 2)	40,23
CdS-600	28,28	(1 0 1)	64,00
	45,79	(1 1 1)	39,02
	47,53	(0 1 3)	38,58
	51,62	(1 1 2)	37,87
	24,88	(1 0 0)	81,35
	26,29	(0 0 2)	81,58
CdS-700	27,99	(1 0 1)	48,16
	43,47	(1 1 0)	37,84
	47,79	(0 1 3)	77,66
	51,51	(1 1 2)	66,31

3.2.3. BAND GAP DETERMINATION

Determination of the band gap of each CdS sample that has been synthesized is done by UV-DRS characterization, where data will be obtained in the form of

absorbance, reflectance, and wavelength. Band gap calculation can use the tauc plot method and the absorbance edge method. Cadmium sulfide is a semiconductor so the calculation of the tauc plot method is done by extrapolating from the graph of the relationship between transmittance (αhv^2) to band gap energy (eV) then forming a straight line to the x-axis (hv) Asadah et al. (2022). The band gap energy graph is shown in Figure 5.

Figure 5

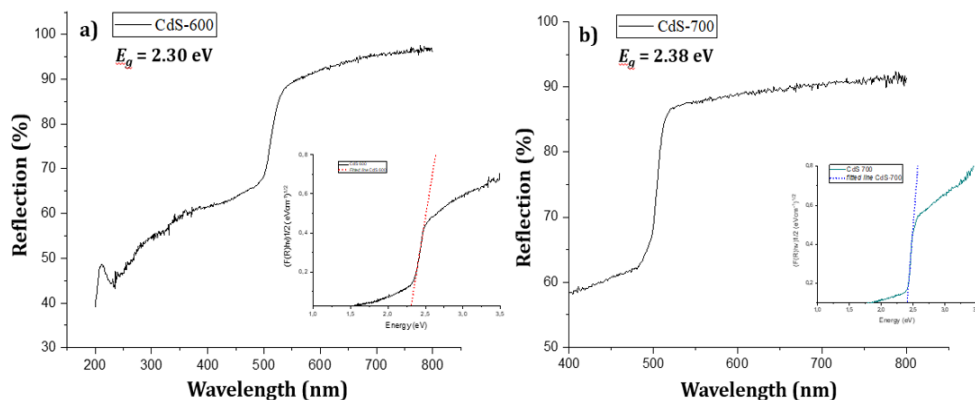


Figure 5 UV-DRS Result Graph of Tauc Plot Method a) CdS-600 and b) CdS-700

Figure 5 shows that the calcination temperature during synthesis affects the band gap energy. The band gap value of CdS-600 is 2.30 eV while the CdS-700 band gap energy is 2.38 eV. Crystal formation is accelerated by the calcination temperature, which allows agglomeration to occur. The shift in absorption can be affected by agglomeration which causes a change in the E_g (band gap energy) value Asadah et al. (2022). The smaller the band gap, the lower the energy required to excite electrons. As a result, the light adsorption of the sample is greater. Increased light adsorption offers better opportunities for photocatalytic applications Asadah et al. (2022).

3.2.4. FUNCTIONAL GROUP ANALYSIS

The peak spectra for the two cadmium sulfide samples, CdS-600 and CdS-700, did not show significant peak shifts, proving that the change in calcination temperature did not affect the functional groups. The absorption peak at 3061 cm^{-1} corresponds to the stretching vibration of hydroxyl group (O-H) adsorbed on the catalyst surface. The absorption peak at 1550 cm^{-1} indicates the presence of C=O asymmetry stretching vibration. Peaks at 1174 cm^{-1} ; 1175 cm^{-1} ; 1070 cm^{-1} ; and 1057 cm^{-1} are related to C=S stretching vibrations derived from sulfide compounds and C-O Kumar & Sharma (2016). Other absorption peaks at 880 cm^{-1} and 883 cm^{-1} are out-of-plane bending vibrations of O-H from H_2O molecules Kumar & Sharma (2016). Typical absorption peaks of Cd-S bond stretching vibrations were observed at peaks below 700 cm^{-1} namely 585 , 588 , 650 , and 652 cm^{-1} Munyai et al. (2021), Bakhsh & Khan (2022). These results indicate that tea leaf extract has a good effect in stabilizing CdS nanoparticles.

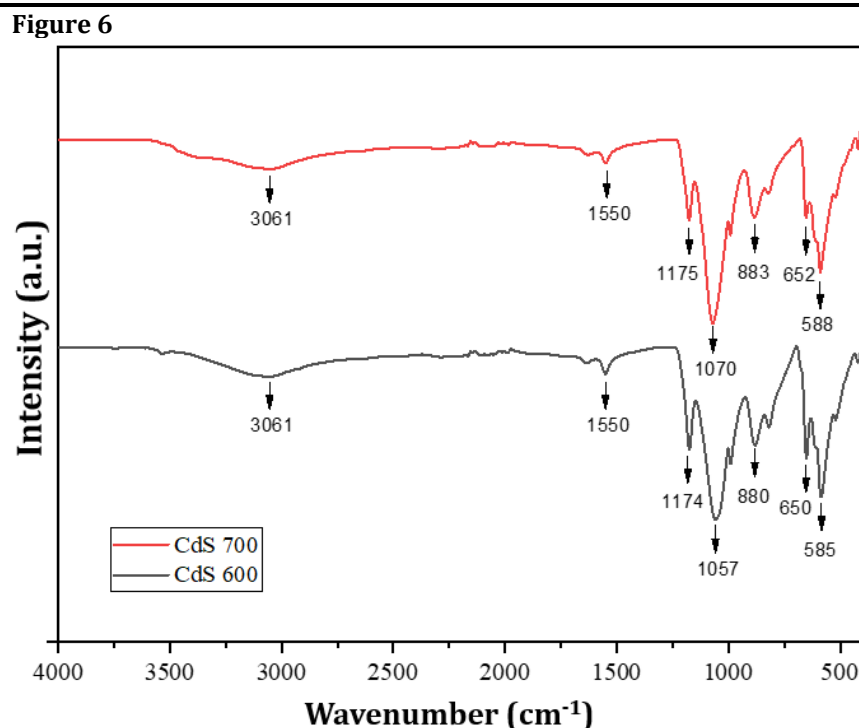


Figure 6 FTIR Spectrum CdS-600 (Black Line) and CdS-700 (Red Line)

3.3. APPLICATION OF CDS FOR CIPROFLOXACIN PHOTODEGRADATION

The photocatalytic degradation in [Figure 7](#) shows that the variation of calcination temperature in the synthesis of cadmium sulfide affects the photocatalytic quality. The three variations of CdS show that the longer the irradiation time of the photocatalyst, the higher the percentage of degradation. This is due to the more energy the electrons get to excite to produce hydroxy radicals. The increasing number of hydroxy radicals will increase the bond-breaking process in organic pollutants, namely ciprofloxacin and is characterized by a decrease in the absorbance of ciprofloxacin [Kumar & Sharma \(2016\)](#).

The degradation of ciprofloxacin by CdS-500 to CdS-600 increased and decreased at CdS-700. The decreased photocatalytic activity can be caused by precipitation on the catalyst during photocatalysis so that there are parts of the catalyst surface that do not absorb photons or ciprofloxacin compounds optimally. Another possibility is that CdS-700 is affected by a decreased surface area. A large surface area will provide more active sites that not only react with absorbed water and hydroxyl to form oxidative hydroxyl radicals but also organic molecules for photodegradation. Generally, the specific surface area increases with decreasing crystal size [Cheng et al. \(2014\)](#) (this is supported by CdS crystal size data by XRD).

The best degradation percentages of each sample namely CdS-500; CdS-600; and CdS-700 were 32.18%; 48.72%; and 8.73%, respectively. The optimum condition of CdS synthesis in photocatalytic degradation of ciprofloxacin in this study occurred at a temperature of 600 °C with a CdS mass of 10 mg, irradiation time for 120 minutes and ciprofloxacin concentration of 25 ppm. The photocatalytic degradation test was carried out to see how effective the photocatalyst activity of the synthesized CdS was in degrading ciprofloxacin at various photocatalytic times.

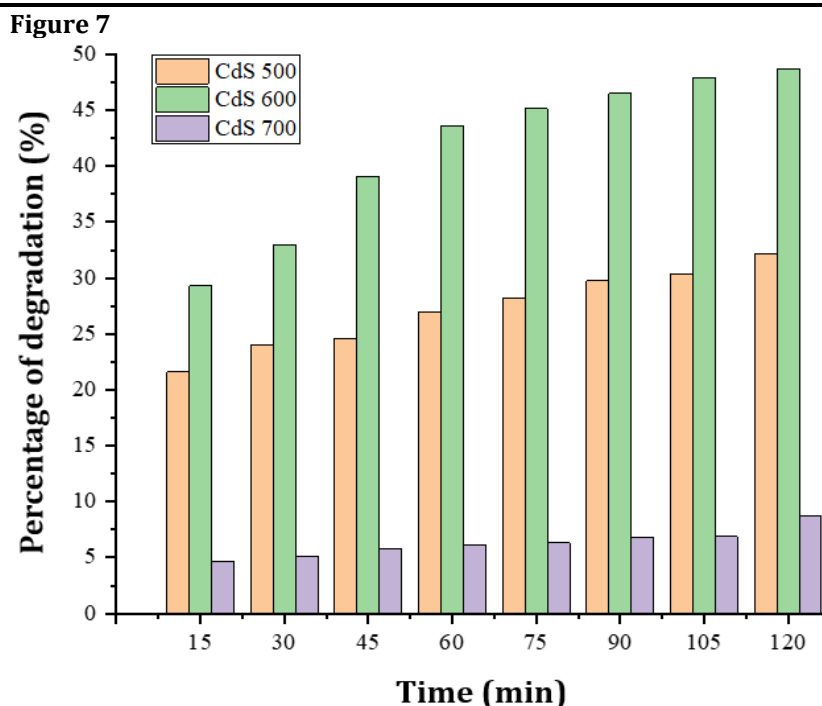


Figure 7 Graph of Degradation Percentage of Ciprofloxacin 25 ppm 100 mL Using CdS 10 mg for Variations of CdS-500; CdS-600; and CdS-700 Against Time.

3.4. REACTION KINETICS OF THE PHOTOCATALYTIC PROCESS

To determine the reaction rate in the photocatalytic degradation of ciprofloxacin by cadmium sulfide with different calcination temperature variations, the respective reaction orders need to be known first. Determination of the pseudo reaction order is done by comparing the coefficient of determination (R^2) value on each CdS variation. The best R^2 value is close to 1 and indicates the order of the reaction that occurs in the photocatalytic degradation of ciprofloxacin. Pseudo-reaction order is used because it only calculates the rate of concentration decrease of ciprofloxacin and not the overall concentration decrease.

Pseudo reaction order is determined by making a graph between the concentration of ciprofloxacin at time t (C_t) against time. A pseudo-first-order reaction is a graph between \ln initial ciprofloxacin concentration (C_0) divided by ciprofloxacin concentration at time t against time. While pseudo-second order is a graph between $(1/C_t) - (1/C_0)$ against time. From the calculation of the reaction order, R^2 data were obtained for each CdS calcination temperature variation which followed the second-order pseudo kinetics. The kinetics curve of ciprofloxacin degradation by cadmium sulfide at various calcination temperatures is shown in [Figure 8](#). Based on the figure, explains that the rate of photocatalytic degradation of ciprofloxacin is the highest on CdS-600. It was found that the reaction rate constants for CdS-500; CdS-600; and CdS-700 were 4×10^{-4} ; 11×10^{-4} ; and $8 \times 10^{-5} \text{ mg}^{-1} \text{Lmin}^{-1}$, respectively. The value of the reaction rate constant depends on several factors, in this study is the initial concentration of ciprofloxacin [Usman et al. \(2021\)](#).

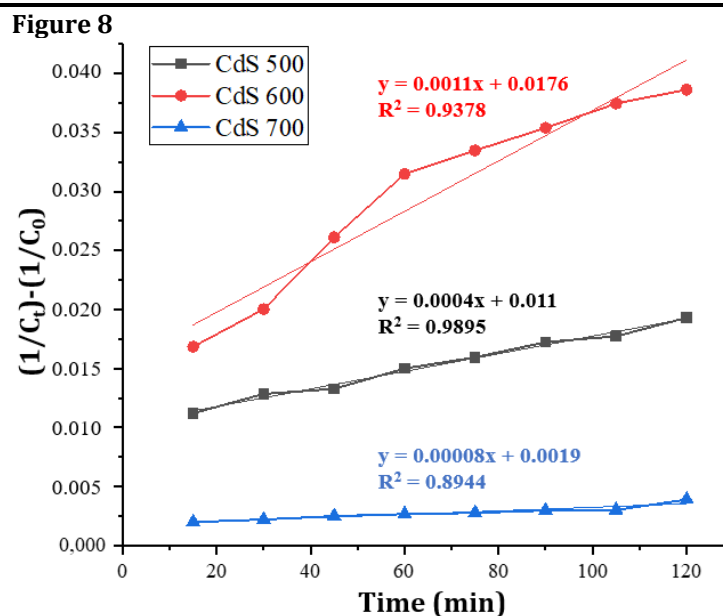


Figure 8 Kinetic Curve of Ciprofloxacin Degradation

4. CONCLUSION

Cadmium sulfide has been successfully synthesized via the green synthesis method with various calcination temperature variations for ciprofloxacin photocatalytic degradation applications. XRD and FTIR characterization results display CdS peaks. SEM-EDX image of the synthesized CdS is smooth round and there are agglomerations with an even distribution of elements. The band gap energy value is influenced by the calcination temperature obtained by CdS-600 of 2.3 eV and CdS-700 of 2.38 eV. Calcination temperature variations affect the size of CdS crystals formed and their band gap energy. Increasing the calcination temperature gives a larger crystal size but the energy of the pit gap increases due to agglomeration which results in a shift in the energy of the band gap. The effectiveness of cadmium sulfide in degrading ciprofloxacin was shown in CdS-600 with a result of 48.72%, CdS-500 at 32.18%, and CdS-700 at 8.73%. Photocatalytic optimal conditions under visible light for 120 minutes with 10 mg of CdS catalyst and an initial ciprofloxacin concentration of 25 ppm. This shows the potential of developing an environmentally friendly antibiotic waste treatment method.

CONFLICT OF INTERESTS

None.

ACKNOWLEDGMENTS

None.

REFERENCES

- Akerdi, A. G., & Bahrami, S. H. (2019). Application of Heterogeneous Nano-Semiconductors for Photocatalytic Advanced Oxidation of Organic Compounds: A Review. *Journal of Environmental Chemical Engineering*, 7(5). <https://doi.org/10.1016/J.JECE.2019.103283>

- Aprilianingrum, F. A. (2016). Optimasi Dan Regenerasi Fotokatalis Ca. Universitas Negeri Yogyakarta.
- Asadah, E., Hadisantoso, E. P., Soni Setiadi, D., Kimia, J., Sains, F., Teknologi, D., Gunung, S., Bandung, D., Nasution, J. A. H., 105 A, N., Cibiru, C., & Jawa Barat, B. (2022). Pengaruh Suhu Kalsinasi Terhadap Sintesis Kadmium Sulfida (Cds) Menggunakan Metode Presipitasi untuk Penanganan Metilen Biru Secara Fotokatalisis. *Gunung Djati Conference Series*, 7, 60–69.
- Bakhsh, E. M., & Khan, M. I. (2022). Clove Oil-Mediated Green Synthesis of Silver-Doped Cadmium Sulfide and Their Photocatalytic Degradation Activity. *Inorganic Chemistry Communications*, 138(November 2021). <https://doi.org/10.1016/j.inoche.2022.109256>
- Barra Caracciolo, A., Topp, E., & Grenni, P. (2015). Pharmaceuticals in the Environment: Biodegradation and Effects on Natural Microbial Communities. A review. *Journal of Pharmaceutical and Biomedical Analysis*, 106, 25–36. <https://doi.org/10.1016/J.JPBA.2014.11.040>
- Chauhan, J. K. R. P. (2020). Effect of Temperature on Properties of Cadmium Sulfide Nanostructures Synthesized by Solvothermal method. *Journal of Materials Science: Materials in Electronics*. <https://doi.org/10.1007/s10854-019-02807-7>
- Cheng, H., Wang, J., Zhao, Y., & Han, X. (2014). Effect of Phase Composition, Morphology, and Specific Surface Area on the Photocatalytic Activity of TiO₂ Nanomaterials. *RSC Advances*, 4(87), 47031–47038. <https://doi.org/10.1039/C4RA05509H>
- Chopra, S., & Kumar, D. (2017). Ibuprofen as an Emerging Organic Contaminant in Environment, Distribution and Remediation. <https://doi.org/10.1016/j.heliyon.2020.e04087>
- Dolatabadi, J. E. N. (2011). Molecular Aspects on the Interaction of Quercetin and its Metal Complexes with DNA. *International Journal of Biological Macromolecules*, 48(2), 227–233. <https://doi.org/10.1016/J.IJBIOMAC.2010.11.012>
- Dsikowitzky, L., & Schwarzbauer, J. (2014). Industrial Organic Contaminants: Identification, Toxicity and Fate in the Environment. *Environmental Chemistry Letters*, 12(3), 371–386. <https://doi.org/10.1007/S10311-014-0467-1/METRICS>
- Gunawan, Adi Wijaya, R., Suseno, A., Lusiana, R. A., Septina, W., & Harada, T. (2023). Synthesis of CuInS₂ thin Film Photocathode with Variation of Sulfurization Sources and Pt-In₂S₃ Modification for Photoelectrochemical Water Splitting. *Journal of Electroanalytical Chemistry*, 945. <https://doi.org/10.1016/J.JELECHEMA.2023.117683>
- Gunawan, G., Megawati, S. G. L., Prasetya, N. B. A., & Wijaya, R. A. (2022). Synthesis, Characterization of Ag₂S from AgCl Waste of Argentometry Titration with Heating Temperature Variations and Its Application as a Temperature Sensor Based on Negative Temperature Coefficient (NTC). *Jurnal Kimia Sains Dan Aplikasi*, 25(8), 292–299. <https://doi.org/10.14710/JKSA.25.8.292-299>
- Gunawan, G., Prasetya, N. B. A., & Wijaya, R. A. (2023). Degradation of Ciprofloxacin (CIP) Antibiotic Waste using The Advanced Oxidation Process (AOP) Method with Ferrate (VI) from Extreme Base Electrosynthesis. *Trends in Sciences*, 20(7). <https://doi.org/10.48048/TIS.2023.6639>
- Kelly, K. R., & Brooks, B. W. (2018). Global Aquatic Hazard Assessment of Ciprofloxacin: Exceedances of Antibiotic Resistance Development and Ecotoxicological Thresholds. *Progress in Molecular Biology and*

- Translational Science, 159, 59–77.
<https://doi.org/10.1016/BS.PMBTS.2018.07.004>
- Kumar, R. N., Sadaf, S., Verma, M., Chakraborty, S., Kumari, S., Poliseti, V., Kallem, P., Iqbal, J., & Banat, F. (2023). Old Landfill Leachate and Municipal Wastewater Co-Treatment by Sequencing Batch Reactor Combined with Coagulation–Flocculation Using Novel Flocculant. *Sustainability (Switzerland)*, 15(10), 8205. <https://doi.org/10.3390/SU15108205/S1>
- Kumar, S., & Sharma, J. K. (2016). Stable Phase CdS Nanoparticles for Optoelectronics: A Study On Surface Morphology, Structural and Optical Characterization. *Materials Science- Poland*, 34(2), 368–373. <https://doi.org/10.1515/MSP-2016-0033>
- Lang, D., Xiang, Q., Qiu, G., Feng, X., & Liu, F. (2014). Effects of Crystalline Phase and Morphology on the Visible Light Photocatalytic H₂-Production Activity of CdS Nanocrystals. *Dalton Transactions*, 43(19), 7245–7253. <https://doi.org/10.1039/C3DT53601G>
- Majumder, S., Gupta, S., & Raghuvanshi, S. (2014). Removal of Dissolved Metals by Bioremediation. *Heavy Metals in Water*, 44–56. <https://doi.org/10.1039/9781782620174-00044>
- Mathur, P., Sanyal, D., Callahan, D. L., Conlan, X. A., & Pfeffer, F. M. (2021). Treatment Technologies to Mitigate the Harmful Effects of Recalcitrant Fluoroquinolone Antibiotics on the Environment and Human Health. *Environmental Pollution*, 291. <https://doi.org/10.1016/J.ENVPOL.2021.118233>
- Munyai, S., Tetana, Z. N., Mathipa, M. M., Ntsendwana, B., & Hintsho-Mbita, N. C. (2021). Green Synthesis of Cadmium Sulphide Nanoparticles for the Photodegradation of Malachite Green Dye, Sulfoxazole and Removal of Bacteria. *Optik*, 247. <https://doi.org/10.1016/J.IJLEO.2021.167851>
- Shehu Imam, S., Adnan, R., & Mohd Kaus, N. H. (2018). Photocatalytic Degradation of Ciprofloxacin in Aqueous Media: A Short Review. *Toxicological & Environmental Chemistry*, 100(5–7), 518–539. <https://doi.org/10.1080/02772248.2018.1545128>
- Shen, L., Liang, S., Wu, W., Liang, R., & Wu, L. (2013). CdS-Decorated UiO-66(NH₂) Nanocomposites Fabricated by a Facile Photodeposition Process: An Efficient and Stable Visible-Light-Driven Photocatalyst for Selective Oxidation of Alcohols. *Journal of Materials Chemistry A*, 1(37), 11473–11482. <https://doi.org/10.1039/C3TA12645E>
- Shivaji, K., Mani, S., Ponmurugan, P., De Castro, C. S., Lloyd Davies, M., Balasubramanian, M. G., & Pitchaimuthu, S. (2018). Green-Synthesis-Derived CdS Quantum Dots Using Tea Leaf Extract: Antimicrobial, Bioimaging, and Therapeutic Applications in Lung Cancer Cells. *ACS Applied Nano Materials*, 1(4), 1683–1693. <https://doi.org/10.1021/acsanm.8b00147>
- Usman, M. R., Prasasti, A., Fajriyah, S., Marita, A. W., Islamiah, S., Firdaus, A. N., Noviyanti, A. R., & Eddy, D. R. (2021). Degradation of Ciprofloxacin by Titanium Dioxide (TiO₂) Nanoparticles: Optimization of Conditions, Toxicity, and Degradation Pathway. *Bulletin of Chemical Reaction Engineering & Catalysis*, 16(4), 752–762. <https://doi.org/10.9767/bcrec.16.4.11355.752-762>
- Verma, V., & Singh, S. V. (2023). Augmentation of Photocatalytic Degradation of Methylene Blue Dye Using Lanthanum and Iodine Co-Doped TiO₂ Nanoparticles, Their Regeneration and Reuse; and Preliminary Phytotoxicity Studies for Potential use of Treated Water. *Journal of*

- Environmental Chemical Engineering, 11(6).
<https://doi.org/10.1016/J.JECE.2023.111339>
- Xiao, J., Wen, B., Melnik, R., Kawazoe, Y., & Zhang, X. (2014). Phase Transformation of Cadmium Sulfide Under High Temperature and High Pressure Conditions. *Physical Chemistry Chemical Physics*, 16(28), 14899–14904. <https://doi.org/10.1039/C4CP01003E>
- Zhao, W., Li, Y., Zhao, P., Zhang, L., Dai, B., Xu, J., Huang, H., He, Y., & Leung, D. Y. C. (2021). Novel Z-Scheme Ag-C₃N₄/SnS₂ Plasmonic Heterojunction Photocatalyst for Degradation of Tetracycline and H₂ Production. *Chemical Engineering Journal*, 405, 126555. <https://doi.org/10.1016/J.CEJ.2020.126555>
- Zhao, Y., Li, Y., & Sun, L. (2021). Recent Advances in Photocatalytic Decomposition of Water and Pollutants for Sustainable Application. *Chemosphere*, 276. <https://doi.org/10.1016/J.CHEMOSPHERE.2021.130201>
- Zhou, G. J., Li, S. H., Zhang, Y. C., & Fu, Y. Z. (2014). Biosynthesis of CdS Nanoparticles in Banana Peel Extract. *Journal of Nanoscience and Nanotechnology*, 14(6), 4437–4442. <https://doi.org/10.1166/JNN.2014.8259>